JOURNAL OF MATERIALS SCIENCE 20 (1985) 3018–3026

Microplasticity in Elgiloy

M. ASSEFPOUR-DEZFULY, W. BONFIELD
Department of Materials, Queen Mary College, Mile End Road, London E1 4NS, UK

The room temperature microstrain characteristics of Elgiloy (composition in wt%, 40 Co, 20 Cr, 15 Ni, 7 Mo, 2 Mn, 0.1 C, balance Fe) have been determined for a range of microstructures corresponding to various alloy treatments reported previously. The friction stress was found to be constant ($\sigma_F = 12 \pm 3\,MN\,m^{-2}$) for the solution treated (after prestrain), cold-worked and cold-worked plus aged at 500° C conditions, but decreased to $\sigma_F = 5 \pm 3\,MN\,m^{-2}$ after ageing at 800° C. The microscopic yield stress (MYS) increased with cold-working and subsequent ageing at 500° C to a maximum value of $210\,MN\,m^{-2}$ reflecting the increase in the long range internal stress field. An increase in the MYS of the solution treated strip was noted with ageing at 800° C, whereas the MYS of the cold-worked samples was decreased by this treatment. The solution treated and aged at 800° C samples exhibited a two-stage stress–plastic microstrain curve, whereas the cold-worked and cold-worked plus aged at 500° C conditions showed a three-stage stress–plastic microstrain behaviour.

1. Introduction

The microstructure of Elgiloy, an alloy of composition in wt%, 40 Co, 20 Cr, 15 Ni, 7 Mo, 2 Mn, O.1 C, balance Fe(15.9), has been characterized recently [1] for the solution treated (ST), 36% cold-worked (36% CW), 72% cold-worked (72% CW) and various age hardened conditions. It was demonstrated that the ST Elgiloy consisted of a single phase solid solution with a fcc austenitic type crystal structure. Cold-rolling of this fcc structure by 36% and 72% created a network of thin lamellae of fcc deformation twins and hcp ε-platelets, which produced substantial strengthening of the alloy. Subsequent ageing of the cold-worked strip at 500° C caused further hardening and this was attributed either to the formation of further hcp ε-phase (via the $\alpha \rightarrow \varepsilon$ transformation) and/or to the possible segregation of zones at platelet interfaces. In contrast the ST condition did not harden significantly at 500° C, but after ageing at 800° C for long periods (~ 1000 h) an increase in hardness was noted due to the formation of a coarse Mo–Co–Cr intermetallic compound. Ageing of the cold-worked strip at 800° C caused an initial softening due to dissolution of the deformation-induced hcp ε-platelets, recovery and recrystallization.

The establishment of a range of microstructures in Elgiloy has some important consequences in one of its major applications, namely as a spring element in inertial navigation instruments. The major mechanical property requirements in such applications are dimensional stability and minimum hysteresis. Hitherto, Elgiloy has been generally utilized in the "cold-worked condition", but the amount of cold-work has not been standardized. The previous study [1] demonstrated, not only that the amount of cold-work has a significant effect on the resultant microstructure, but that subsequent ageing can also produce significant microstructural changes.

In this paper, the room temperature mechanical properties associated with the range of possible microstructures are reported, with particular reference to the microstrain characteristics associated with relatively small dislocation movements.

2. Experimental procedure

Strips of Elgiloy were supplied by the Royal

0022–2461/85 $03.00 + .12

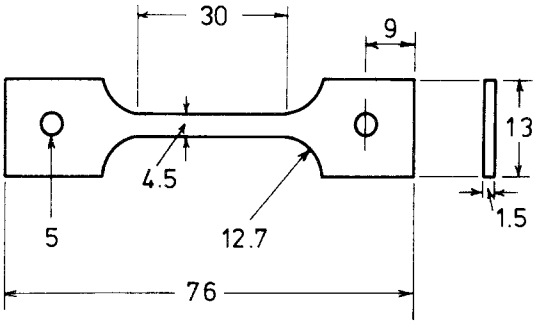

Figure 1 Microstrain tensile test specimen. Dimensions in mm.

Aircraft Establishment in the 36% CW and 72% CW conditions and the ST condition was prepared by a solution treatment of the cold-worked strip for 1 h at 1300° C followed by water quenching. Tensile specimens of rectangular cross-section were machined from the strip, the dimensions of which are shown in Fig. 1, and given various ageing treatments, as listed in Table I. The specimens were electropolished prior to testing, in a solution of 5% perchloric acid in acetic acid at $T < 30°$ C and a voltage of 50 to 60 V, to remove the machining marks and oxide films formed on the surface during heat treatment.

The microstrain behaviour was determined with a capacitance strain gauge [2]. A load–unload technique [3, 4], at a strain rate of $3 \times 10^{-5}\,\text{sec}^{-1}$, was used to measure the friction stress (σ_F), the microscopic yield stress (MYS), defined as the stress required to produce a plastic strain of 2×10^{-6}, and the rate of strain hardening in the microstrain region ($d\sigma/d\varepsilon$), which refers to the slope of the stress–plastic microstrain curve. The stress for gross microyielding (σ_m), was taken for comparison purposes as the stress to produce a plastic strain of 100×10^{-6}, and can be considered as an approximate measure of the onset of macroscopic flow. However, it should be noted that for some conditions relatively large strain increments were produced at plastic strains less than 100×10^{-6}. MYS, $d\sigma/d\varepsilon$ and σ_m were measured directly from the stress–plastic microstrain curves, whereas σ_F was calculated from the closed hysteresis loops which were obtained at stress levels below MYS, by the following procedures [5]:

(a) from a plot of loop area (W), against maximum loop width ε_p, with

$$W = 2\sigma_F\varepsilon_p \quad (1)$$

(b) from a plot of loop area (W), against maximum applied loop stress (σ), with σ_F calculated from the extrapolation to $W = 0$, when

$$\sigma = \sigma_E = 2\sigma_F \quad (2)$$

with σ_E = elastic limit.

3. Results

3.1. Hysteresis loops

On the first loading of the solution treated (ST) condition, open loops were traced immediately after the elastic limit (σ_E), prior to which linear elastic behaviour was exhibited as shown in Fig. 2 and closed hysteresis loops were obtained only after prestraining of the ST samples. For all

TABLE I Hardness and microstrain data

Specimen condition	Hardness (VHN)	σ_F = Slope/2 (± 3 MN m^{-2})	$\sigma_F = \frac{1}{2}\sigma_E$ (± 3 MN m^{-2})	MYS (MN m^{-2}) $\varepsilon_p = 2 \times 10^{-6}$	σ_m (MN m^{-2}) $\varepsilon_p = 100 \times 10^{-6}$
ST	200	–	–	35	160
ST 0.05% prestrained	200	12	9	100	160
36% CW	340	12*	9*	70	275
72% CW	440	12	9	155	670
36% CW aged 64 h at 500° C	400	12*	9*	80	625
72% CW aged 5 h at 500° C	510	12	9	210	895
ST aged 1263 h at 800° C	280	5	5	158	210
72% CW aged 1263 h at 800° C	310	5	5	75	322

*Not shown in Figs. 4 to 7.

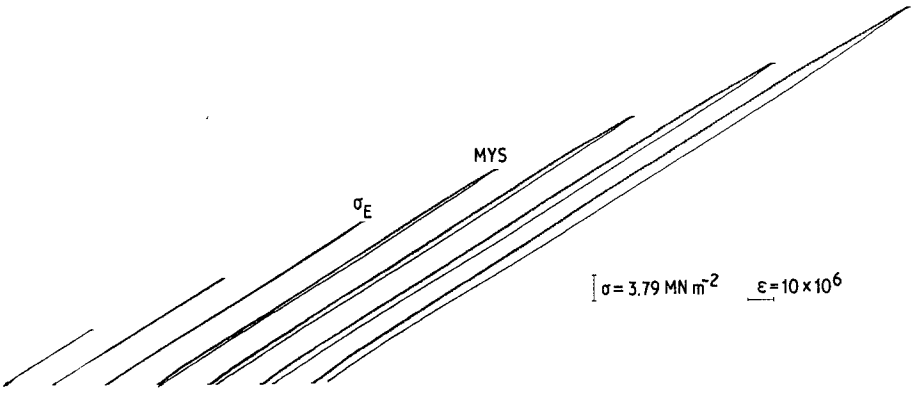

Figure 2 Hysteresis loops for ST condition.

the other conditions of Elgiloy investigated, closed hysteresis loops were traced on the first loading of the specimen above the elastic limit, σ_E, as shown in Fig. 3. As the stress was increased progressively above σ_E, larger closed loops were traced, with the loop area increasing with stress amplitude, until the anelastic limit, σ_A, was reached at which an open loop was observed, indicating that plastic deformation had occurred.

3.2. Friction stress

The friction stress, σ_F, for various alloy conditions was calculated from the initial linear slopes of plots of loop area W, against loop width, ε_p, examples of which are shown in Figs. 4 and 5. The friction stress was found to be approximately constant ($\sigma_F \simeq 12$ MN m^{-2}) for the ST 0.05% prestrained, cold-worked and cold-worked plus aged at 500° C conditions (Fig. 4), whereas the samples aged at 800° C (Fig. 5) had a lower friction stress ($\sigma_F \simeq 5$ MN m^{-2}). Lack of experimental data points at small loop widths (i.e. loop width $< 3 \times 10^{-6}$) in Fig. 5 introduces some uncertainty in the initial slope of the curve and hence in σ_F. However, the values of W in the loop width range from 3 to 6 $\times$ 10^{-6} in Fig. 5, indicate a lower friction stress for the samples aged at 800° C. This conclusion is also supported by

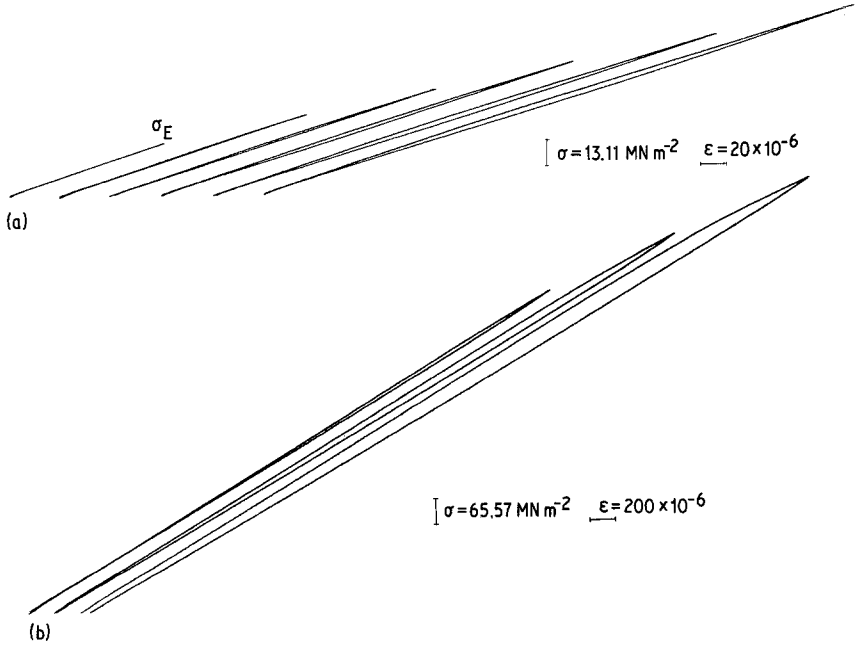

Figure 3 (a) Hysteresis loops for 72% CW, aged 5 h at 500° C condition, showing initial elastic behaviour, followed by closed loops at stresses greater than the elastic limit, σ_E. (b) As (a), but at higher stresses showing closed loops followed by an open loop at σ greater than the anelastic limit, σ_A (i.e. $\sigma >$ MYS).

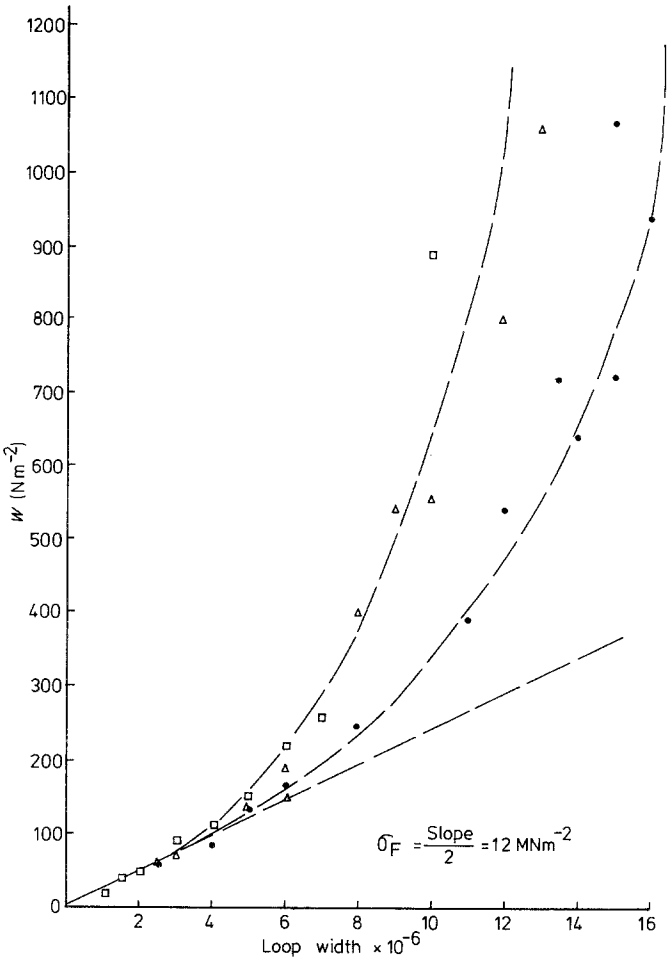

Figure 4 Loop area, W, against loop width, ε_p. ● ST 0.05% prestrained, △ 72% CW, □ 72% CW aged 5 h at 500° C.

graphs of loop area, W, against maximum loop stress, σ (Figs. 6 and 7) which give a lower value of the elastic limit, σ_E, and therefore a lower σ_F (as $\sigma_E = 2\sigma_F$) for the samples aged at 800° C. Reasonable agreement exists between the σ_F values obtained from both Equations 1 and 2, as shown in Table I.

A deviation from linear behaviour is noted at higher stress amplitudes in both the W against ε_p (Figs. 4 and 5) and W against σ (Figs. 6 and 7) curves, a result which will be considered in the next section.

3.3. Microscopic yield stress and microplastic deformation

The stress–plastic microstrain curves determined by plotting the maximum loop stress, σ, against the total plastic strain, $\varepsilon_{p,total}$, are shown in Figs. 8 and 9, for various conditions of the alloy. The MYS values obtained by a direct reading of the plastic microstrain from the first open loop, could also be deduced from these curves by identifying the stress corresponding to a strain of 2×10^{-6}, as listed in Table I for all the treatments investigated. The MYS of $\sim 35\,MN\,m^{-2}$ for the ST condition was increased to about $100\,MN\,m^{-2}$ when the specimen was prestrained by $\sim 0.05\%$. The 36% CW sample had a MYS of $\sim 70\,MN\,m^{-2}$, while the MYS of the 72% CW strip was substantially higher at about $155\,MN\,m^{-2}$.

Ageing of the 36% CW sample at 500° C up to peak hardness (64 h) increased the MYS only slightly to about 80 MN m^{-2}, whereas ageing of the 72% CW strip for 5 h at 500° C (peak hardness) increased the MYS significantly to about 210 MN m^{-2}.

Ageing of the ST sample at 800° C, increased the MYS value in a similar manner to the hardness values previously reported [1], with an MYS of ~ 158 MN m^{-2} obtained for the peak hardness condition (1263 h at 800° C). Ageing of the

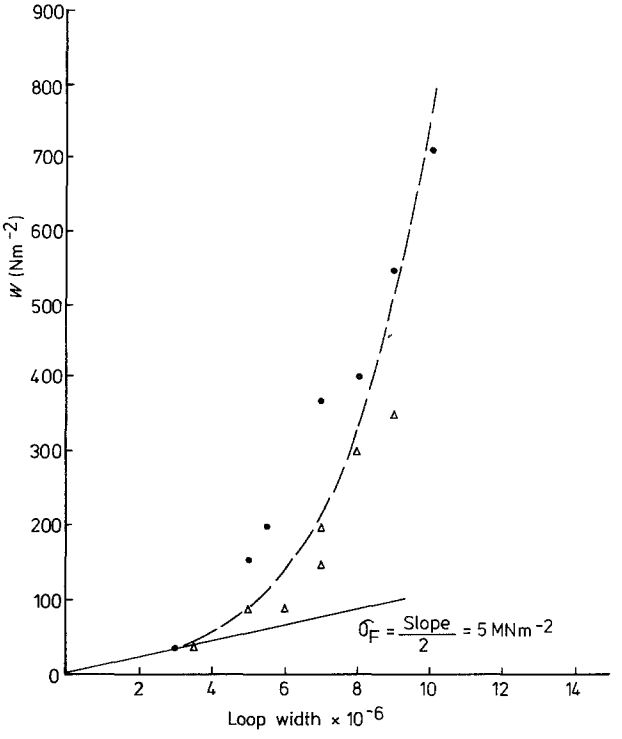

Figure 5 Loop area, W, against loop width, ε_p. ● ST aged 1263 h at 800° C, △ 72% CW aged 1263 h at 800° C.

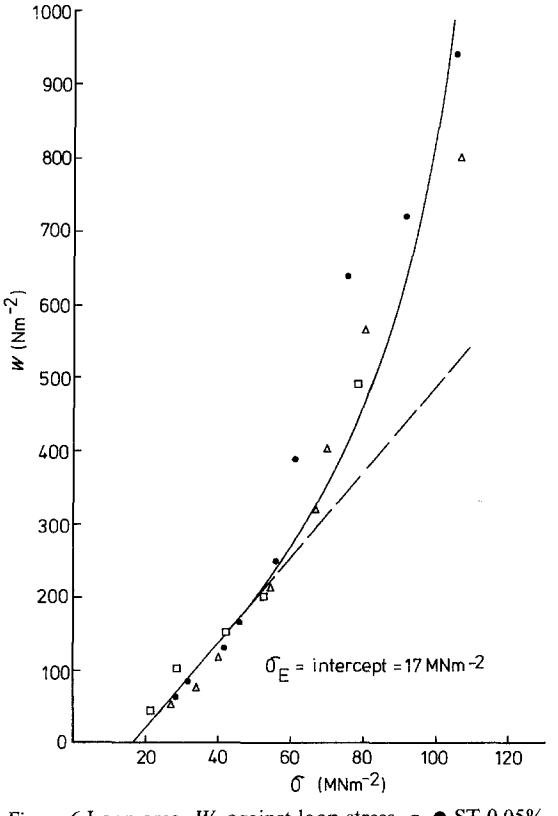

Figure 6 Loop area, W, against loop stress, σ. ● ST 0.05% prestrained, △ 72% CW, □ 72% CW aged 5 h at 500° C.

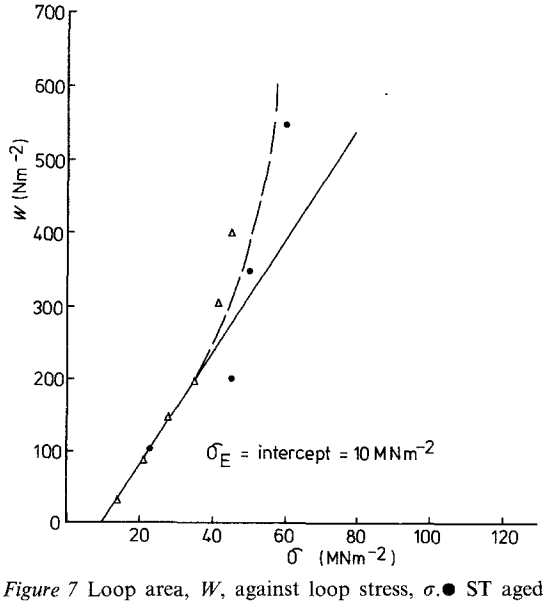

Figure 7 Loop area, W, against loop stress, σ.● ST aged 1263 h at 800° C, △ 72% CW aged 1263 h at 800° C.

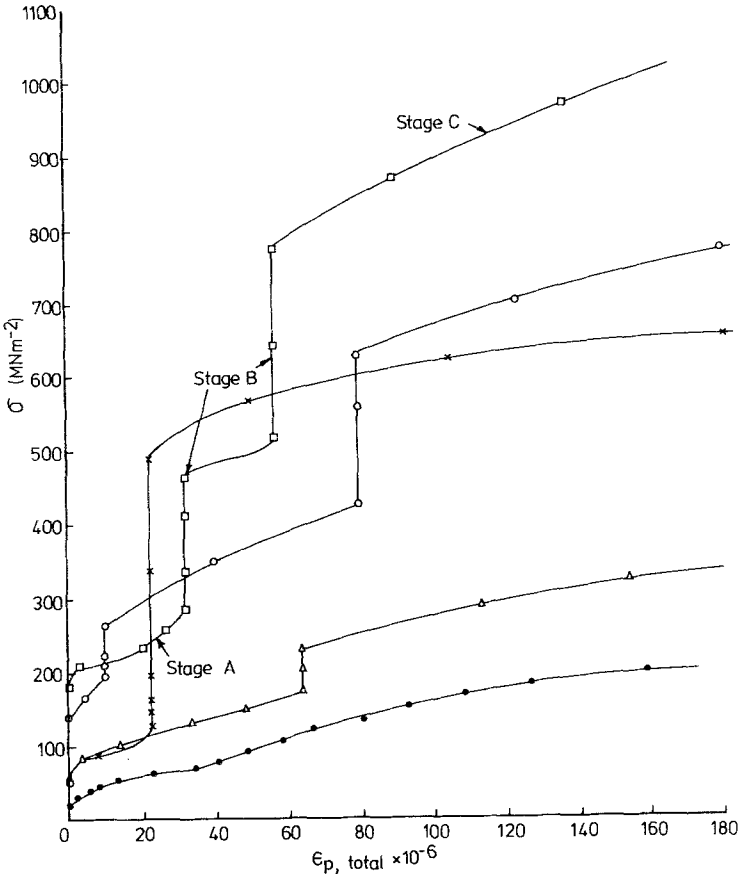

Figure 8 Stress, σ, against plastic strain, $\varepsilon_{p.total}$. ● ST, ○ 72% CW, □ 72% CW aged 5 h at 500° C, △ 36% CW, × 36% CW aged 64 h at 500° C.

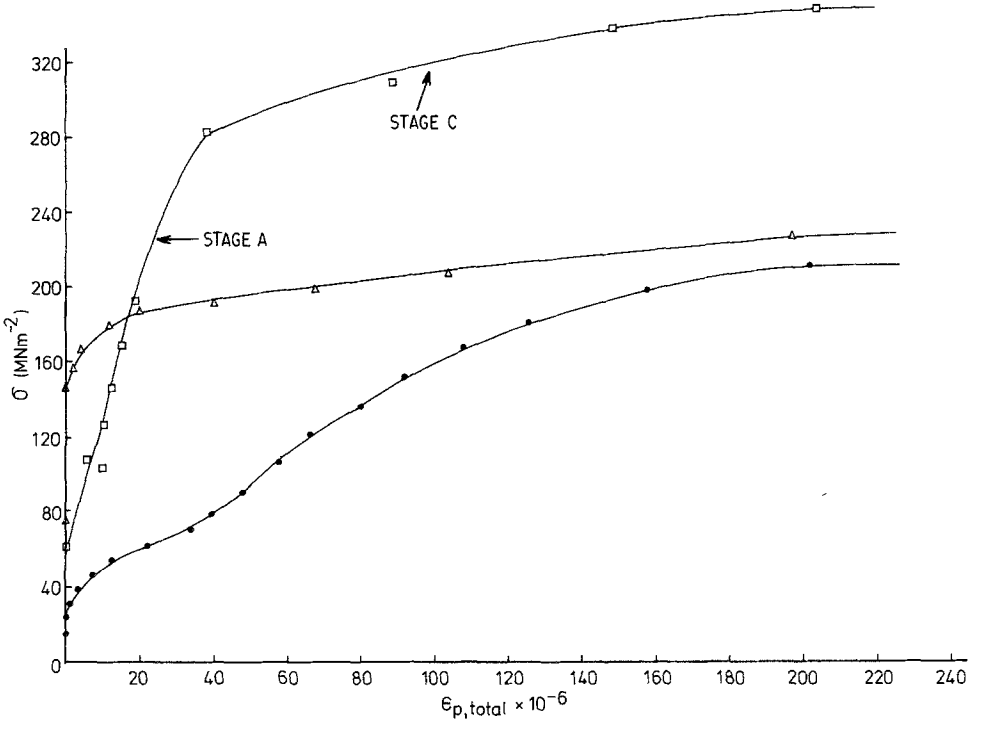

Figure 9 Stress, σ, against plastic strain, $\varepsilon_{p.total}$. ● ST, △ ST aged 1263 h at 800° C, □ 72% CW aged 1263 h at 800° C.

72% CW strip at 800° C, on the other hand, reduced the MYS value of ~155 MN m^{-2} to about 75 MN m^{-2} after 1263 h at this temperature, again similar to the hardness variation noted for this condition [1].

The rate of strain hardening in the microstrain region followed either two or three distinctive stages of behaviour, depending on the alloy condition, as shown in Figs. 8 and 9. The values of the stress (σ_m) defining the onset of the region of gross microyielding, i.e. when relatively large plastic strains are produced by small additional stress increments, are listed in Table I.

3.4. Macrostrain data

Macrostrain parameters, such as the ultimate tensile stress (UTS) and percentage elongation to fracture (%e), determined from the conventional load–elongation curves are given in Table II, for various conditions of Elgiloy. %e was determined from both the load–elongation curve, and direct measurement on the tensile specimen after fracture.

Cold-working the ST strip by 36%, reduced %e with an accompanying increase in the UTS (Table II). In the 72% CW strip, the %e to fracture was substantially reduced (compared to the ST and 36% CW) with a corresponding increase in the UTS.

Ageing the 36% CW and 72% CW samples at 500° C to peak hardness (64 h and 5 h, respectively, produced further drops in %e, together with more increases in the UTS.

The macrostrain properties deteriorated with ageing of the ST strip at 800° C, with a reduction in %e to fracture, as well as a small decrease in the UTS. Ageing of the 72% CW sample at 800° C, increased the %e to fracture, with a corresponding decrease in the UTS.

TABLE II Macrostrain data

Specimen condition	UTS (MN m^{-2})	%e
ST	780	80
36% CW	890	60
72% CW	1330	10
36% CW aged 64 h at 500° C	978	40
72% CW aged 5 h at 500° C	1500	7
ST aged 1263 h at 800° C	750	14
72% CW aged 1263 h at 800° C	1030	36

4. Discussion

When specimens in the ST condition were first loaded beyond the elastic limit (σ_E), open loops, indicating plastic deformation, were observed (Fig. 2), but closed hysteresis loops were formed after prestraining. Similar findings have been reported in several metals in the fully annealed condition [6–10] and are attributed to a relatively low dislocation density in which isolated dislocations could move irreversibly at stresses greater than σ_E, and hence produce an open loop. For a closed hysteresis loop, the elastic restoring forces from the line tension and internal stress field (σ_μ) must be sufficient to restore the dislocations to their original positions, a condition which is achieved only after a certain amount of prestraining which establishes a back stress on the dislocations equal to or greater than the friction stress, σ_F, i.e. the dislocations have to be moved far enough to make $\sigma_\mu \gtrsim \sigma_F$. In the cold-worked samples, the internal stress field is relatively large and closed hysteresis loops were obtained immediately after the elastic limit (Fig. 3) through the reversible bowing of dislocation segments.

The friction stress, σ_F, for the various conditions of Elgiloy, calculated from the initial slope of the W against ε_p curves, was found to be constant (within the experimental error range) for the ST plus prestrain, cold-worked and cold-worked plus aged at 500° C conditions ($\sigma_F = 12 \pm 3$ MN m^{-2}). This result indicates that the friction stress is independent of the h c p ε-phase and f c c twin platelets which form within the f c c lattice after 36% and 72% cold-working [1]. It is concluded that the energy dissipation process occurs by the reversible movement of dislocations in the networks present within the platelet-free region of the f c c matrix and does not involve any interactions with the platelets. The friction stress therefore appears as a constant regardless of the amount of cold-deformation (or subsequent ageing at 500° C) and as such, is dependent on the intrinsic lattice resistance to dislocation motion (Peierls stress) once a dislocation network is established after some predeformation.

The friction stress of samples aged for long periods at 800° C (both ST and cold-worked

conditions) was $\sigma_F = 5 \pm 3$ MN m^{-2}, which is about half the value obtained for all the other conditions examined. Precipitation of the intermetallic Mo–Co–Cr compound after ageing at 800° C is accompanied by a change in the composition of the f c c matrix [1]. Solid solution hardening of the matrix provided by molybdenum (and to some extent chromium) is reduced when these elements form the intermetallic precipitate and the intrinsic lattice resistance to dislocation motion, and consequently the friction stress, are reduced.

The elastic limit, σ_E, was calculated by extrapolating the initial linear region of the W against σ curves to zero loop area ($W = 0$), and the equation $\sigma_E = 2\sigma_F$ was used to calculate σ_F. The σ_F values obtained in this way are in reasonable agreement with those determined from the slope of W against ε_p curves (Table I).

The friction stress, σ_F, is considered as the lowest value of the short range effective stress (σ^*) in accordance with the analysis of Lukas and Klensil [5], and is thought to represent the average of those stresses opposing dislocation motion, which dissipate energy irreversibly during the generation of a closed hysteresis loop. A deviation from linear behaviour is observed in the W against ε_p, curves at higher stress amplitudes (also in the W against σ curves), as shown by the upward positive curvature following the linear region (Figs. 4 to 7). This departure from linearity at high stress levels has been reported in the literature for most of the metals and alloys investigated, and it is to be expected as Equation 1 is strictly applicable only in the limit as $\varepsilon_p \to 0$ (i.e. in the initial region of low stress amplitudes). Furthermore, at high strain amplitudes the dislocations experience other energy dissipative mechanisms, as they move over relatively greater distances in the lattice [11].

In constrast to σ_F, MYS is related to the stress required to overcome the maximum amplitude of the internal stress field [12], and therefore, the general increase in MYS with cold-working and ageing (Table I) can be explained in terms of an increase in the amplitude of the long range internal stress field. In the cold-worked samples this increase in the amplitude of the long range internal stress field is due to the formation of deformation twins and h c p ε-platelets, and in the cold-worked plus aged at 500° C condition a further increase is caused by the formation of additional h c p ε-phase and/or the segregation of molybdenum atoms at platelet interfaces. In the ST aged at 800° C condition the formation of the Mo–Co–Cr intermetallic compound causes an increase in MYS, whereas the MYS of the 72% CW sample is reduced by ageing at 800° C due to dissolution of the h c p ε-platelets (the f c c structure is stable at high temperature [1]), which causes a decrease in the amplitude of the long range internal stress field.

The two-stage stress–plastic strain behaviour exhibited by the ST condition and samples aged at 800° C (Fig. 9) has been reported for a number of annealed metals [13–15]. Stage A represents the initial stage of work hardening and is believed to indicate the rate at which a few dislocation sources are activated, i.e. a dislocation exhaustion mechanism is thought to be operating during stage A. In stage C, in which relatively large plastic strains are produced by small additional stress increments (gross microyielding), the applied stress level is considered to be high enough to create a large number of mobile dislocations by activating many dislocation sources.

The three-stage stress–plastic microstrain curve exhibited by the cold-worked and cold-worked plus aged at 500° C samples (Fig. 8), has also been reported in annealed polycrystalline nickel [16], Cu–1.9 wt % Be precipitation hardening alloy [13] and cold-worked Ni-span C [17]. Stages A and C are controlled as previously described.

Stage A is considered to represent the movement of dislocations through areas which are essentially free of h c p ε-platelets. As the dislocations move over larger distances with increasing stress, they interact with the twin and h c p ε-platelets in the cold-worked material, represented by stage B. The coherent twin and h c p ε-platelets act as effective obstacles to dislocation motion and account for the substantial increase in the rate of strain hardening during stage B. This is envisaged to occur via the interaction of dislocations with the coherency strain fields at the matrix/platelet interfaces and the subsequent pile-ups of dislocations against these barriers. The increase in length and slope of stage B with increasing cold-working (i.e. for the 72% CW specimen) is attributed to the increase in the density of the platelets and a

corresponding decrease in the inter-platelet spacing. Similarly, ageing of the cold-worked samples at 500° C substantially increases the length of stage B through an increase in the effective obstacle density and coherency strain fields.

Stage C is correlated with a substantial increase in the mobile dislocation density as many dislocation sources are activated, together with the onset of cross-slip of the platelets by the piled-up dislocations. In the 36% CW and 36% CW plus aged at 500° C specimens, the strain hardening rate in stage C is similar to the ST condition, whereas that for the 72% CW and 72% CW aged at 500° C samples is higher due to the greater platelet density.

Similarly, the enhancement of the macroscopic mechanical properties (such as the UTS and hardness) by cold-working and subsequent ageing at 500° C, is attributed to the deformation twins and h c p ε-platelets acting as effective barriers to dislocation motion. In contrast, the loss of ductility, produced by ageing of the ST and cold-worked strips at 800° C is related to the coarse and brittle Mo–Co–Cr intermetallic compound formed at this temperature [1].

5. Conclusions

1. The friction stress, σ_F, of Elgiloy was found to be approximately constant ($\sigma_F = 12 \pm 3$ MN m^{-2}) for the ST (after prestrain), cold-worked and cold-worked plus aged at 500° C conditions, and is considered to reflect the intrinsic lattice resistance of the matrix. The friction stress decreased to $\sigma_F = 5 \pm 3$ MN m^{-2} after long time ageing of ST and cold-worked specimens at 800° C, an effect attributed to the loss of solid solution strengtheners, molybdenum and chromium, from the matrix in the formation of the Mo–Co–Cr intermetallic compound.

2. The MYS increased with cold-working and subsequent ageing at 500° C as a consequence of the increase in the amplitude of the long range internal stress field produced by the formation of twins and h c p ε-platelets and a general increase in dislocation density. Ageing of the ST strip at 800° C, also caused an increase in MYS, associated with the formation of Mo–Co–Cr intermetallic precipitate, whereas ageing the 72% CW samples at 800° C caused a decrease in MYS associated with dissolution of h c p ε-platelets and recrystallization and recovery.

3. A two-stage stress–plastic microstrain curve was observed for the ST, ST aged at 800° C, and cold-worked aged at 800° C conditions, whereas a three-stage stress–plastic microstrain behaviour was exhibited by the cold-worked, and cold-worked plus aged at 500° C samples.

Acknowledgements

The authors gratefully acknowledge the provision of a University of London Studentship for M. Assefpour-Dezfuly together with the helpful support of Mr C. R. Milne, Radio and Navigation Division, Royal Aircraft Establishment in the supply of Elgiloy specimens.

References

1. M. ASSEFPOUR-DEZFULY and W. BONFIELD, *J. Mater. Sci.* **19** (1984) 2815.
2. W. BONFIELD, P. K. DATTA, B. C. EDWARDS and D. C. PLANE, *ibid.* **8** (1973) 1832.
3. W. BONFIELD and C. H. LI, *Acta Metall.* **11** (1963) 585.
4. *Idem, ibid.* **13** (1965) 317.
5. P. LUKAS and M. KLENSIL, *Phys. Status Solidi* **11** (1965) 127.
6. J. M. ROBERTS and N. BROWN, *Trans. Met. Soc. AIME* **218** (1960) 454.
7. J. M. ROBERTS and N. BROWN, *Acta Metall.* **10** (1962) 430.
8. J. M. ROBERTS and D. E. HARTMAN, *Trans. Met. Soc. AIME* **230** (1964) 1125.
9. N. BROWN and R. A. EKVALL, *Acta Metall.* **10** (1962) 1101.
10. R. KOSSOWSKY and N. BROWN, *ibid.* **14** (1966) 131.
11. A. LAWLEY and J. D. MEAKIN, *ibid.* **14** (1966) 236.
12. H. CONRAD, *J. Metals* **16** (1964) 582.
13. W. BONFIELD, *Trans. Met. Soc. AIME* **239** (1967) 99.
14. A. R. ROSENFIELD and B. L. AVERBACH, *Acta Metall.* **8** (1960) 624.
15. C. W. MARSCHALL and R. E. MARINGER, "Dimensional Instability" (Pergamon Press, Oxford, 1977).
16. R. D. CARNAHAN and J. E. WHITE, *Philos. Mag.* **10** (1964) 513.
17. O. K. JOSHI, PhD thesis, University of London (1977).

Received 12 September
and accepted 25 October 1984